Estimation of the mechanism of consecutive hard starts in bipropellant thrusters

Yoshiki Matsuura*† and Yasuhito Kano*, Satoshi Ikegami*, Erica Uchiyama*, Yu Daimon**, Kohji Tominaga**

* IHI Aerospace Co., Ltd.

900 Fujiki, Tomioka, Gunma, Japan

** Japan Aerospace Exploration Agency (JAXA)

2-1-1 Sengen, Tsukuba, Ibaraki, Japan

† Corresponding Author: Yoshiki Matsuura, yoshiki-matsuura@iac.ihi.co.jp

Abstract

Hypergolic bipropellant engines, commonly used for orbital maneuvers and attitude control of spacecraft, ignite through the impingement of liquid-phase oxidizer and liquid-phase fuel. In firing tests simulating space operation, conducted in high-altitude test stands capable of achieving low-pressure environments of several hPa, a phenomenon known as "hard start" is occasionally observed. During a hard start, the combustion chamber pressure rises abruptly to several times the nominal operating pressure. This phenomenon is believed to occur when propellants are injected into the combustion chamber at extremely low pressure, causing flash boiling and forming a premixed gas mixture. Ignition occurs when liquid-phase oxidizer and fuel injection begins simultaneously, leading to detonation. Furthermore, all the propellants in the combustion chamber are consumed instantaneously, resulting in a temporary flameout. It was observed that hard starts could repeat in situations where the supply pressure of the propellants temporarily decreases due to the effects of water hammer. This phenomenon is presumed to occur when a portion of the combustion gases backflows into the manifolds, creating a gas-liquid multiphase state of combustion gases and propellants within the manifolds. This recreates a condition similar to the initial engine start-up, resulting in another hard start. To suppress the occurrence of this phenomenon, a design that minimizes the manifold volume is effective. This allows for the rapid expulsion of gas phases from the manifold and ensures that it is quickly filled with liquid-phase propellants, reducing the likelihood of backflow and repeated hard starts.

1. Introduction

Hypergolic propellants, which ignite spontaneously upon impingement of the oxidizer and fuel, eliminate the need for igniters, thereby simplifying the propulsion systems of spacecraft. Consequently, they are widely utilized in various space applications [1]. Among the numerous combinations of hypergolic propellants, the most commonly employed is composed of hydrazine or its derivatives as the fuel and dinitrogen tetroxide (N_2O_4 , Oxidizer, NTO) as the oxidizer. The applications of hypergolic propellants are extensive, including engines for satellite and orbital transfer vehicles, thrusters for attitude control [2], and landing systems for celestial bodies [3]. Consequently, the required thrust levels can vary depending on the specific application.

In the development of new engines, the initial focus is typically on several critical factors: confirming the ability to achieve stable combustion at a steady thrust level, ensuring that the temperature throughout the engine remains within the allowable limits of the materials utilized, and attaining the target-specific impulse. Moreover, to manage development costs effectively, combustion tests are generally conducted in atmospheric pressure environments during the initial stages of development. As engine development advances and the complexity of the engine increases, the focus typically shifts to evaluating ignition characteristics in high-altitude pressure environments and assessing vacuum thrust performance. The selection of hypergolic propellants fundamentally addresses many concerns regarding successful ignition. However, during engine startup in high-altitude pressure environments, the internal flow paths used for injecting propellants into the combustion chamber can approach near-vacuum conditions. This phenomenon inevitably results in some evaporation of the incoming propellants, resulting in impinging conditions between the oxidizer and fuel, which differ from those observed in atmospheric firing tests. Depending on the engine design, this can lead to excessive ignition delay times or a sudden and steep increase in ignition pressure. The significance of

bipropellant thrusters and engines utilizing hypergolic propellants has been reaffirmed as a propulsion technology capable of adapting to increasingly complex orbital operations. This type of hypergolic bipropellant thruster must be engineered to accommodate not only continuous operations spanning several thousand seconds but also pulse operations that require rapid ignition and extinguishment within a timeframe of 10 to 100 ms. The rise in the combustion chamber pressure—and consequently, the timing of thrust rise—varies between the initial combustion event and subsequent combustions during such pulse operations [4,5]. Furthermore, widely recognized instances of hard starts exist, where ignition during pulse combustion can generate shock pressures several times greater than the steady-state combustion pressure of the thruster [4,6]. This raises significant concerns regarding the need to mitigate impact loads on both the thruster and the spacecraft, as well as the potential for initiating unstable combustion [7]. To efficiently advance engine development, the ignition characteristics in high-altitude pressure environments should be considered from the initial design stages. Therefore, a comprehensive understanding of the sequence of events from the opening of the propellant supply valve, through the flow of propellants into the injector, to ignition within the combustion chamber—is essential. This study investigates the transient ignition process through visual observations within the combustion chamber of a small combustor, complemented by measurements of the combustion chamber pressure. Based on these findings, guidelines for engine design that consider ignition characteristics are proposed in this study.

2. Experimental setup

In a bipropellant impinging-type combustor, the initial processes of liquid film formation, liquid thread development, and droplet formation by the impinging elements, as well as the mixing, evaporation, and ignition of the two propellants occur in an extremely brief timeframe. Furthermore, during ignition in space, all flow paths downstream of the propellant valves are subjected to the orbital pressure conditions, which approximate a near-vacuum state. Upon the opening of the propellant valves, the flow of propellants generates a gas-liquid mixture influenced by their respective vapor pressure characteristics. This phenomenon is anticipated to significantly impact the injection state of the propellants and the formation of impinging elements. To analyze the transient ignition process, combustion tests were conducted using an injector and combustion chamber designed to produce a thrust of approximately 22 N, utilizing MON-3 (NTO blends with 2.5-3.0% NO, Oxidizer) as the oxidizer and hydrazine as the fuel.

Throughout this series of tests, combustion tests were conducted by switching between two types of combustion chambers for a single injector, depending on the specific objectives of the experiments. The first combustion chamber is designed for high-sensitivity pressure measurement, aimed at capturing the transient behavior of pressure within the chamber during ignition with exceptional sensitivity and minimal response delay. The pressure sensor is strategically positioned on the inner surface of the combustion chamber, and it operates at a data recording frequency of 50 kHz. In contrast, the second combustion chamber is specifically designed for visualization purposes. Its primary objective is to visually capture the propellant injection behavior immediately before ignition, as well as the transition from ignition to stable combustion. To facilitate this, the region immediately following the propellant injection is constructed from quartz glass. Both combustion chambers share a cylindrical structure and throat, with identical dimensions in terms of length (measured from the injection surface to the throat), diameter, volume, and throat diameter. The high-sensitivity pressure measurement chamber and visualization chamber are configured with a common setup, utilizing an absolute pressure sensor connected through a pressure conduit to perform measurements at 2 kHz. This shared configuration allows for consistent comparisons across different tests. In the visualization test, a Photron FASTCAM NOVA S16 high-speed camera was used to capture visible light of the entire visualization chamber at 25,000 fps. The test setup is shown in Figure 1, indicating the test specimens employed for the visualization tests. To comprehensively evaluate the process from a low-vacuum state within the combustion chamber and downstream propellant flow paths to ignition and stable combustion, a vacuum chamber of sufficient volume has been integrated downstream of the combustor. This design minimizes pressure fluctuations caused by combustion gases during the firing process, which lasts for a few seconds. The propellant supply system is shown in Figure 2. In the propellant supply system, pressure measurement ports were strategically installed at the inlets of the propellant valves to facilitate real-time monitoring of pressure dynamics. The oxidizer side was designated as PIO, whereas the fuel side was labeled as PIF. This configuration allows for a comprehensive evaluation of the pressure drop behavior during the opening of the propellant valves. The injector was designed to incorporate three phases of oxidizer-fuel impingement pairs, complemented by six phases of fuel injection ports for cooling the inner wall of the combustion chamber. This arrangement not only enhances the mixing of the propellants but also ensures effective cooling of the inner wall of the combustion chamber, with all components evenly distributed circumferentially.

For the hot firing tests, the oxidizer-to-fuel (O/F) mixture ratio was set at 0.8, and the supply pressure was adjusted to achieve a flow rate that generates a thrust of 22 N during stable combustion. The temperatures of the propellant within the supply tank, supply piping, injector, and combustor were maintained at 20°C±3°C. During the firing tests, visualization recording commenced immediately before test initiation. The fuel-side propellant valve was activated at

the 5-s mark, whereas the oxidizer-side propellant valve was opened either simultaneously with the fuel-side valve or 30 ms earlier. This approach was designed to capture variations in transient ignition behavior based on the timing of the oxidizer filling the propellant flow path.

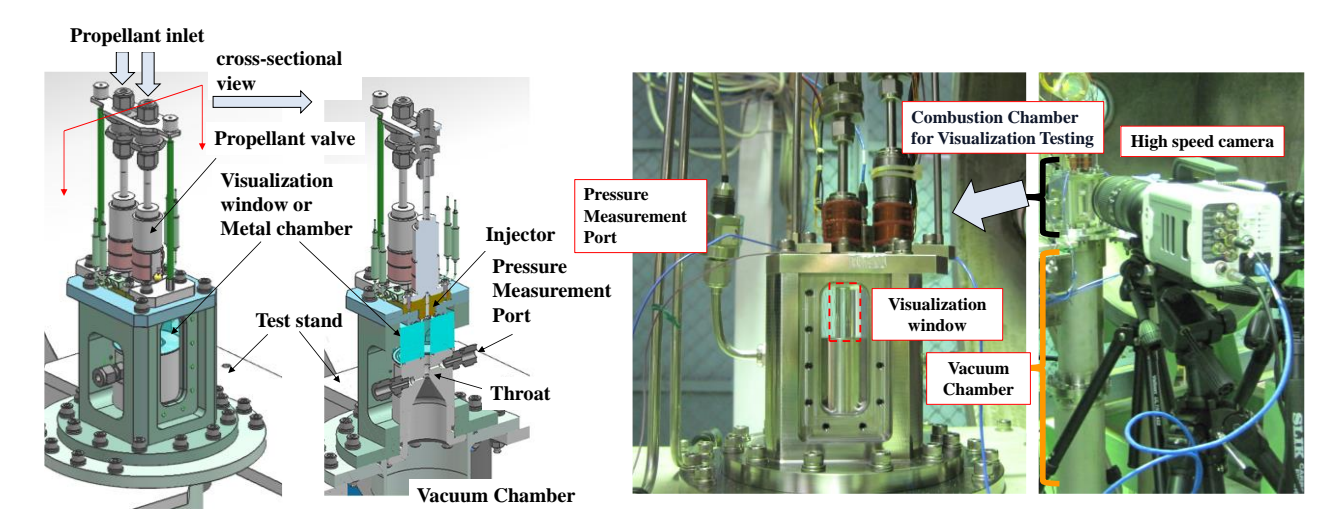


Figure 1: Visualization test equipment and test conditions [4][5]

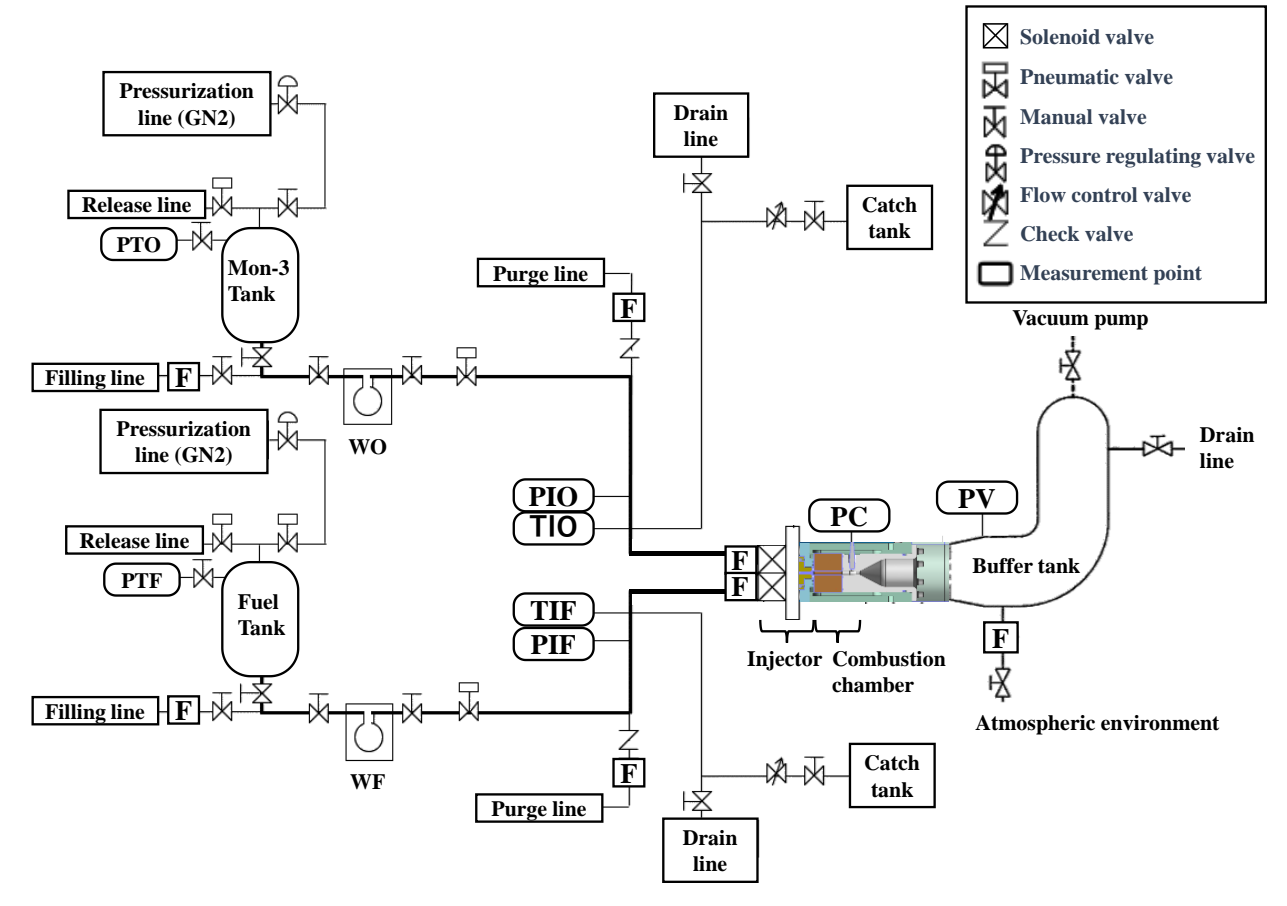


Figure 2: Supply system diagram

3. Experimental result

The combustion-chamber pressure during the high-sensitivity pressure measurement test is shown in Figure 3. A comparison of the results detected by the absolute pressure sensor, which operates at a recording rate of 2 kHz, and the differential pressure sensor, which operates at a recording rate of 50 kHz, reveals a notable response time delay in the absolute pressure sensor. This delay is attributed to the measurement process through the pressure conduit. Additionally, while the 2 kHz pressure sensor could not fully capture the rapid changes in pressure, the 50 kHz differential pressure sensor detected a sharp increase in pressure, with the peak pressure reaching approximately 10 MPa. The positioning of the differential pressure sensor on the inner surface of the combustion chamber facilitates highly sensitive measurements, allowing for the observation of several key phenomena:

- ➤ The combustion chamber pressure initially increases to approximately 0.03 MPaA and stabilizes at this level for a duration of approximately 5.006–5.009 s.
- ➤ The pressure then increases to near approximately 0.1 MPaA, which aligns with the vapor pressure of the oxidizer at 20°C conditions (Figure 4) (approximately 5.010–5.012 s).
- Subsequently, a sharp pressure increase to approximately 0.1 MPaA was detected (5.012 s).

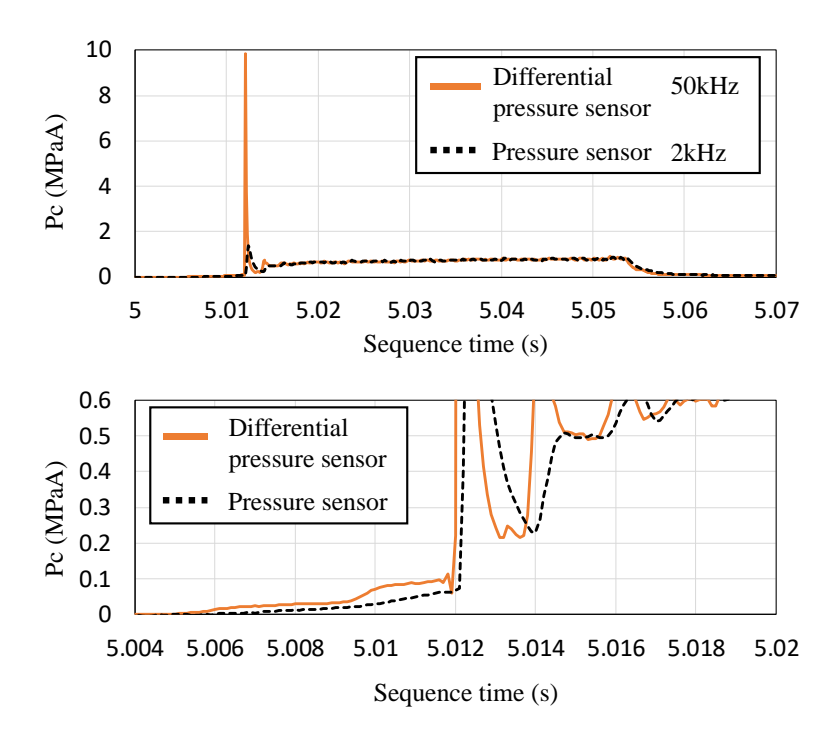


Figure 3: History of combustion chamber pressure

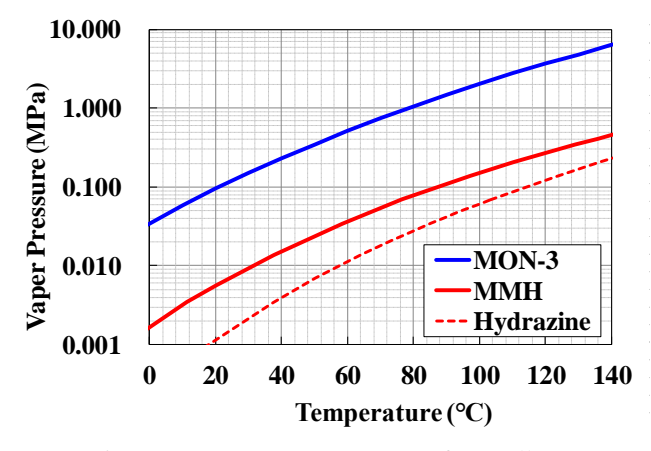


Figure 4: Vapor pressure curve of propellants

A comparison of the histories of the combustion chamber pressure and inlet pressures (PIO and PIF) during the highsensitivity pressure measurement and visualization tests is shown in Figure 5. In each case, a pronounced pressure surge, indicative of a hard start, is observed at the moment of ignition, followed by a transition to steady combustion. Notably, variations were observed in the ignition delay, behavior during the transition to steady combustion, and timing. In the visualization test, the ignition delay leading up to the first hard start was notably shorter. Additionally, this test revealed a pattern of multiple hard starts, which prolonged the transition to steady pressure compared with the highsensitivity pressure measurement test. The difference between the two experimental outcomes are attributed to the difference in the behavior of the propellant supply pressures (PIO and PIF). At a sequence time of approximately 5.005 s, the opening of the propellant valve initiated the flow of propellant into the injector, thereby decreasing PIO and PIF. Differences between the two tests were observed in the magnitude of this drop and the period of pressure oscillations caused by the water hammer within the piping. In the visualization test, a retest was conducted with the initial supply pressure slightly reduced (Figure 6). The ignition delay was approximately 10 ms from the valve-opening signal, which aligned closely with the observations in Figure 5, and multiple ignitions were replicated similarly. When comparing the test results, the behavior of the PIF prior to ignition demonstrated a high degree of similarity between Figure 5 and Figure 6. Conversely, a notable difference was observed in the drop magnitude of PIO immediately before ignition, with the drop magnitude being less pronounced in Figure 6 than that in Figure 5. Based on these observations, the similarity in PIF behavior is likely associated with the occurrence of multiple ignitions. Furthermore, a test was conducted in which the timing of opening the oxidizer propellant valve was advanced by 30 ms relative to the timing of opening the fuel propellant valve, with the intention of reducing the gas-phase ratio inside the oxidizer manifold prior to the initial ignition (Figure 7). In Figure 7, the timing of opening the fuel-side propellant valve is set as time = 0.0. During the initial ignition, the PIO exhibited a significant pressure rise due to the water hammer effect, which was markedly different from the conditions shown in Figure 5 and Figure 6. Under these conditions, multiple ignitions were reproduced, confirming that the level of PIO during the initial ignition was not sensitive to the occurrence of multiple ignitions. On the other hand, the number of multiple ignitions decreased, suggesting a potential sensitivity to the gas-phase ratio inside the oxidizer manifold.

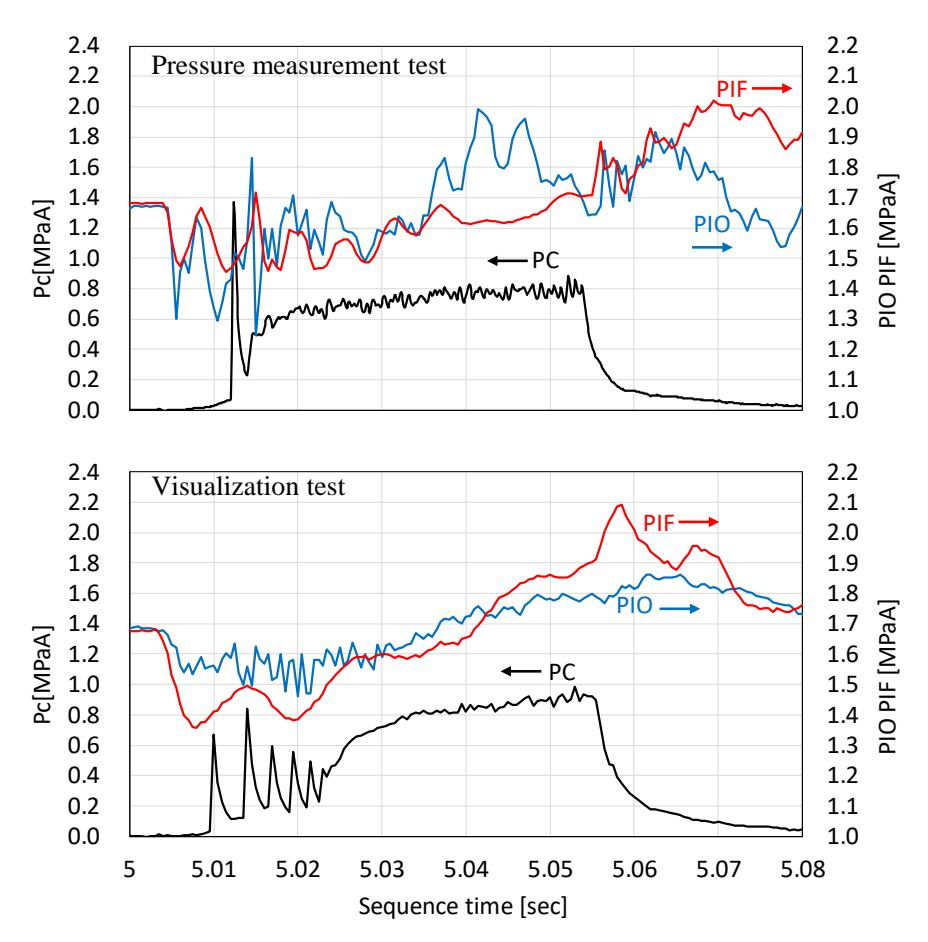


Figure 5: Comparison of pressures history between the pressure measurement test and the visualization test.

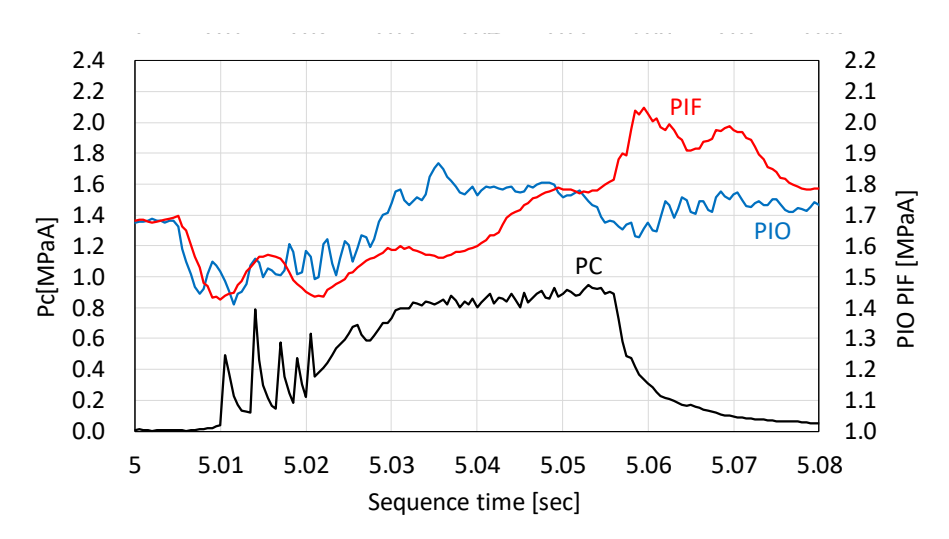


Figure 6: Pressure history in the visualization test with reduced inlet pressure.

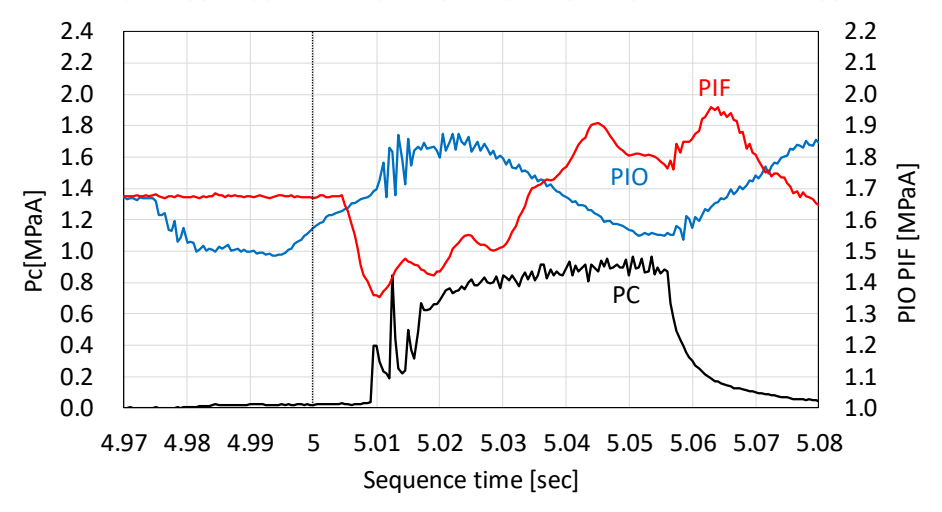


Figure 7: Visualization test with a 30 ms oxidizer lead injection.

The transition process from a hard start to steady combustion is shown in Figure 8, utilizing pressure measurement results and high-speed camera images. When the combustion pressure was approximately 0.03 MPaA, the visualization images maintained a high degree of transparency. As the pressure increased toward 0.1 MPaA, the opacity gradually increased. Eventually, a distinct liquid film formed on the inner surface of the window glass, accompanied by downstream cloudiness, which is presumed to result from the reaction of the two liquids [5,6]. This phenomenon resulted in a hard start. In the visualization test, it has been confirmed that ignition with intense brightness repeatedly occurs during the steep pressure rise indicative of a hard start. (Figure 9). Immediately after the full-area emission in the visualization region triggered by the hard start, no liquid film was observed on the glass surface. Approximately 0.5 ms later, the formation of a liquid film by the fuel resumed, as captured in the visualization (Figure 10). Upon achieving stable combustion, no full-area emissions were observed in the visualization region, and the liquid film remained intact on the wall surface (Figure 11).

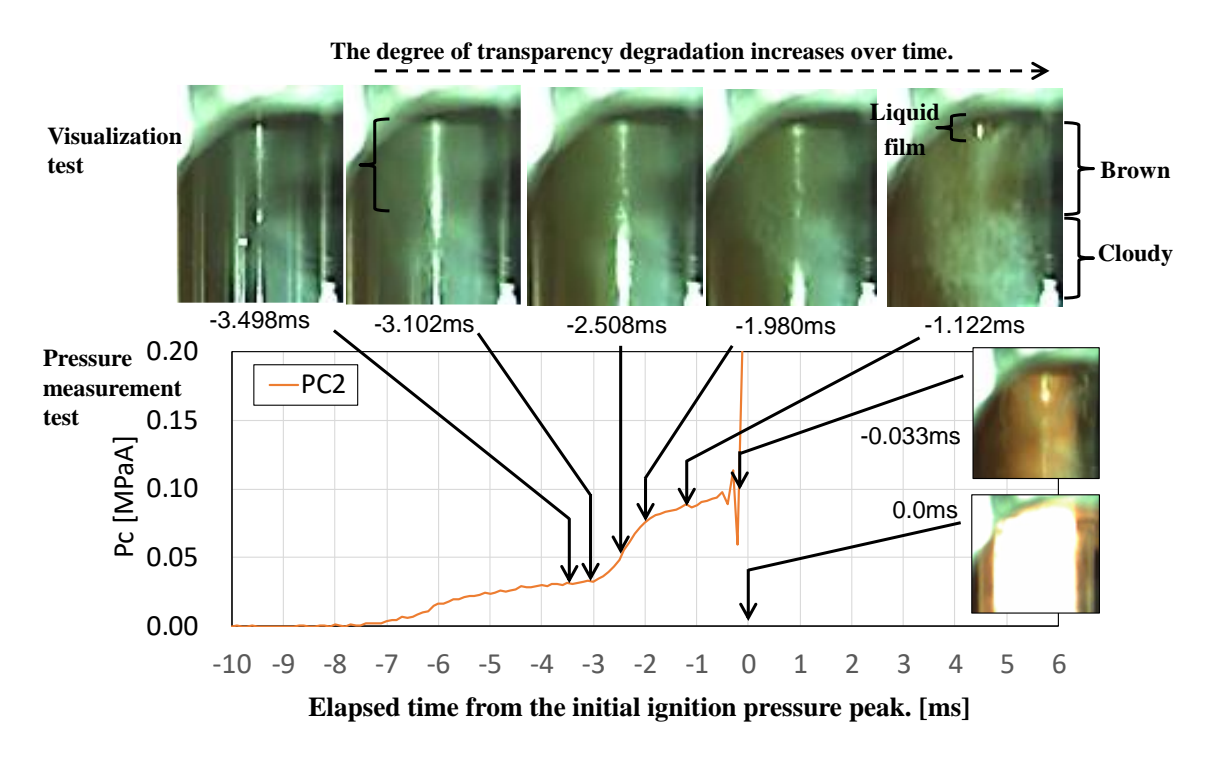


Figure 8: Comparison of pressure history and visualization images during the first ignition. (The time of the pressure peak during the initial ignition was set as the starting point for the elapsed time.)

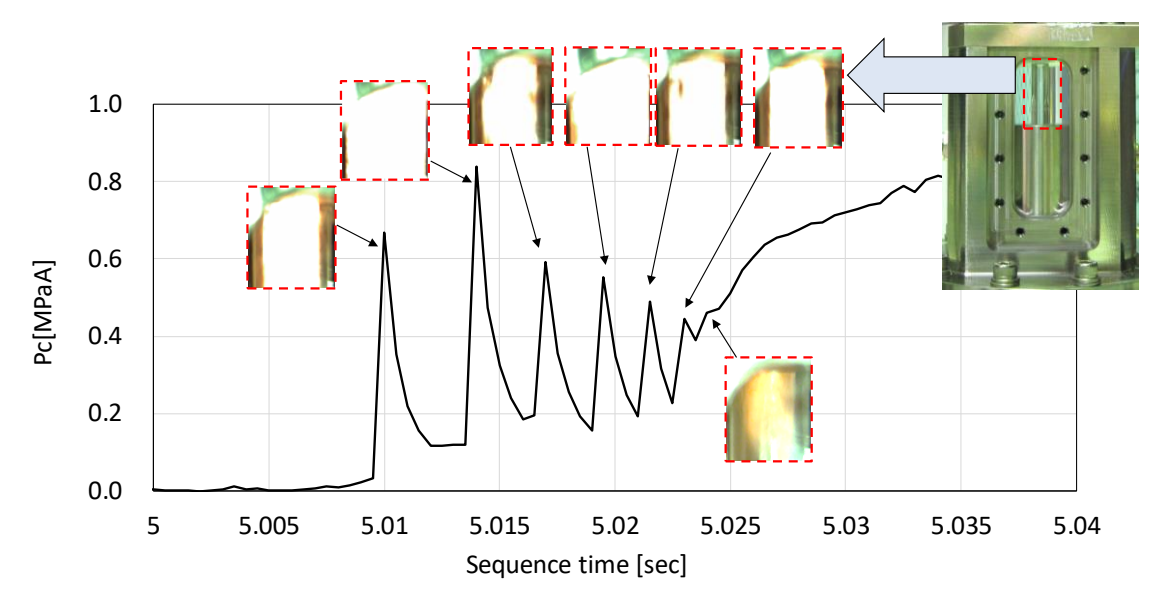


Figure 9: Repeated ignition with intense brightness.

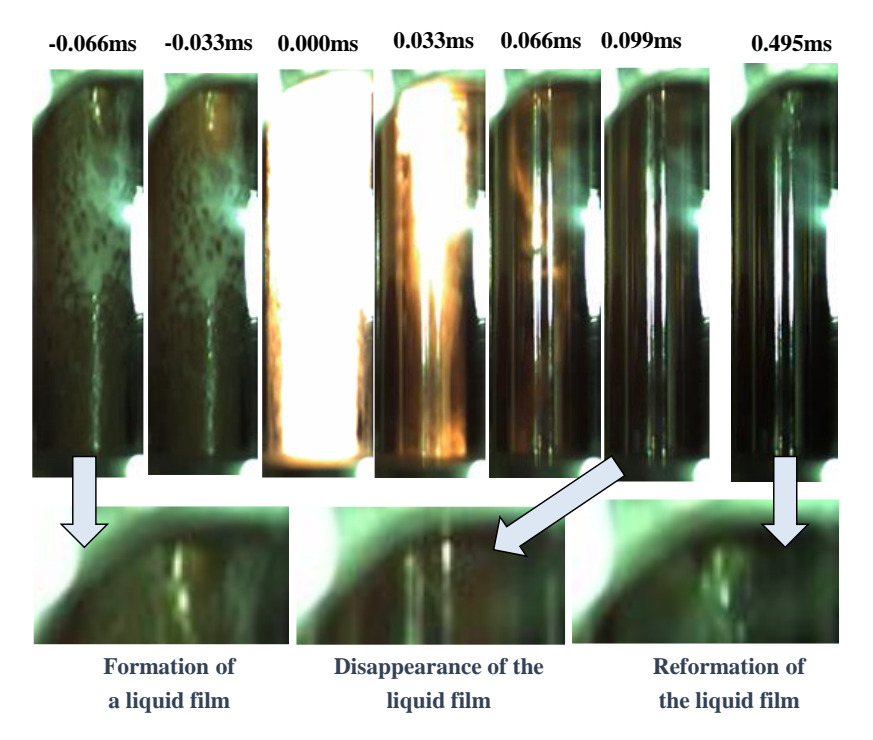
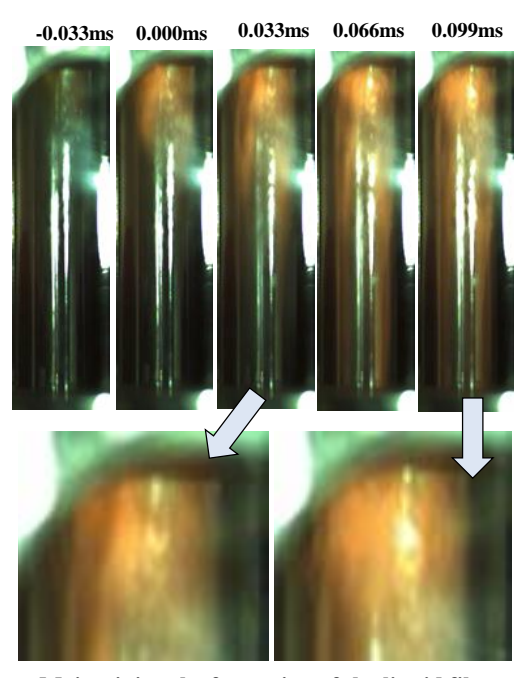


Figure 10: Visualization images before and after the hard-start.

(The timing of the intense emission caused by ignition was set as the starting point for the elapsed time.)



Maintaining the formation of the liquid film

Figure 11: Transition from the seventh ignition to steady combustion.

(The timing of the intense emission caused by ignition was set as the starting point for the elapsed time.)

4. Discussion

The physical mechanism that facilitated ignition from a vacuum state in a bipropellant-impinging-type combustor can be summarized as follows [4, 8-9].

- 1. Hypergolic propellants ignite upon direct contact between the liquid oxidizer and fuel.
- 2. When the propellant valves open, the propellant flows into the propellant flow paths within the injector, which are maintained in a vacuum state. A portion of the propellant evaporates because of flash boiling, consequently increasing the flow path pressure.
- 3. The vapor generated within the injector flow paths is injected into the combustion chamber, causing the chamber pressure to increase until it equilibrates with the exhaust rate through the throat. Concurrently, the pressure within the injector flow paths stabilized at a value corresponding to the injection differential pressure.
- 4. Owing to its high vapor pressure, the oxidizer generates a significant amount of vapor until flash boiling ceases, effectively filling the flow paths with this vapor. Subsequently, two-phase injection (vapor and liquid) continuous until the vapor in the flow paths is entirely replaced by liquid. The liquid-phase oxidizer introduced into the combustion chamber partially evaporated until the chamber pressure reached the oxidizer vapor pressure.
- 5. In the fuel flow path, as the combustion chamber pressure increased, the oxidizer gas infiltrated from the combustion chamber, thereby increasing the pressure within the flow path. Owing to the lower vapor pressure of the fuel compared with that of the oxidizer, flash boiling ceased earlier than in the case of the oxidizer. Consequently, liquid-phase fuel continued to flow into the path, ultimately filling it entirely and initiating liquid-phase injection.
- 6. During the liquid-phase injection of fuel, the oxidizer, existing in a gas-liquid two-phase state, interacts with the fuel. This interaction resulted in a relatively gradual chemical reaction and an increase in the combustion chamber pressure. Eventually, when the pressure within the combustion chamber exceeded the vapor pressure of the oxidizer, the oxidizer transitioned into liquid-phase injection.
- 7. When a sufficient level of liquid-phase oxidizer jet is formed, the two liquids with high momentum impingement, leading to ignition. Prior to this ignition, unburned fuel accumulated within the combustion chamber, and its rapid combustion upon ignition resulted in a phenomenon known as hard start. Consequently, the maximum pressure achieved during the hard start escalated in proportion to the amount of accumulated fuel.

This mechanism is characteristic of the initial ignition and can explain the abrupt pressure increase observed in Figure 5 during the initial ignition. However, it does not fully account for the phenomenon of repeated hard starts that occur multiple times. Reference [9] provides additional insights, including visual observations and pressure history corresponding to point 7 of the aforementioned mechanism. Based on the correlation between the flame propagation speed and CJ-detonation velocity calculated by NASA-CEA, the hard start can be considered a detonation. Reference [10] provides high-speed imaging evidence of recurrent occurrence of abrupt ignition, which led to the cessation of liquid-phase injection for both propellants. This interruption was followed by a resumption of injection and subsequent re-ignition during tests conducted under atmospheric pressure conditions with a combination of NTO and hydrazine. The rapid pressure increase and its propagation during ignition momentarily dispersed the liquid-phase propellants present in the combustion chamber, thereby preventing the impingement of the liquid-phase jets of the oxidizer and fuel. Conversely, the propellant within the flow path remains entirely in the liquid phase. Moreover, the high pressure in the supply tank, combined with the inertia of the flowing liquid, continually drove the propellant through the orifice toward the discharge side. Only one injection orifice exists; thus, the combustion gas pressure generated during ignition does not halt the propellant flow through the orifice. Consequently, the liquid-phase injection rapidly resumes from a state in which the liquid phase is still present at the tip of the injection orifice outlet. At the moment corresponding to the impingement time dictated by the injection flow velocity, the liquid phases impinge once more, resulting in another abrupt ignition observed. While this explanation was not explicitly articulated in [10], it serves as an interpretation of the observed phenomena based on the obtained images and spatial relationships described in the accompanying text. To compare the observations in [10] with those from this study, the visualization test images were analyzed based on the following the steps.

- A) The times required for the propellant to reach the impingement point from the orifice tip are listed in Table 1.
- B) The elapsed time from each hard start to the next pressure increase was validated using the images (Figure 12).
- C) The duration from the burnout of the liquid film layer on the glass window surface, caused by each hard start, to the reformation of the liquid film layer, is shown in Figure 13.

Based on the findings of the above analysis, the following mechanism was proposed, with the sequence of events shown in Figure 14.

- I. The elapsed time until re-ignition was significantly longer than the anticipated re-impingement time, which is calculated based on the assumed flow velocity of the propellant reinjected from the orifice tip. This observation suggests that immediate liquid-phase re-impingement did not occur. The timing of MMH liquid-phase injection, estimated from the reformation of the film cooling liquid layer and observed significantly earlier than re-ignition, indicates a substantial delay in the restart of MON-3 liquid-phase injection.
- II. The timing of the reformation of the film-cooling liquid layer on the visualization window of the combustion chamber, following the third hard start, corresponds with the time required for the liquid to traverse the distance from the injection surface to the wall at the designed injection flow velocity of 0.21 ms. This suggests that the injection resumed from a state in which the fuel was already present at the tip of the orifice for the film injection. Conversely, the reformation of the liquid film after the initial and second hard starts exceeded 0.29 ms, corresponding to the time required for the film-cooling fuel to reach the wall, considering the orifice length and the distance from the injection surface to the wall. This observation indicates that the combustion gases have backflowed into the manifold. The variation in backflow can be attributed to the differences in supply pressure drop, as shown in Figure 5–7. Two types of orifices exist on the outlet side relative to the fuel inlet flow path within the fuel manifold: core injection orifices, which impinge on the oxidizer to generate the primary combustion flame, and film injection orifices, which are utilized for film cooling. Typically, the flow rate designated for film cooling is lower, resulting in a smaller cross-sectional area for the film injection orifices compared with that of the core injection orifices. Consequently, the load applied to the orifice holes owing to the pressure during a hard start differed between the core and film-injection orifices. If the inlet pressure remains sufficiently high, the pressure within the manifold increases accordingly, and inertia forces act to prevent the fuel within the injection orifices from reversing in response to the pressure rise on the outlet side. On the other hand, when the supply pressure experiences a significant drop and the manifold pressure cannot be maintained at an adequate level, it is hypothesized that combustion gases backflow through the core injection orifices, which have larger flow path areas. This backflow then spreads into the film-injection orifices, leading the fuel within the orifices being expelled.
- III. Similarly, it is considered that backflow also occurred on the MON-3 side. During the transition from vapor-dominated injection—triggered by flash boiling at startup—to liquid-phase-dominated injection, ignition is believed to have occurred. As a result, some oxidizer vapor likely remained within the manifold. Because the residual oxidizer vapor is highly compressible, the high pressure generated by the hard start can lead to a substantial backflow of combustion gas into the manifold. This results in a mixed state within the manifold, comprising combustion gases, oxidizer vapor, and liquid-phase oxidizer, thereby creating a gas-liquid two-phase injection condition. Notably, the timing for re-ignition is longer than the reformation of the liquid layer of the fuel film, which is influenced by the re-injection of fuel. This observation indicates that the transition of the oxidizer back to a liquid-phase-dominated injection requires more time than that of the fuel. This suggests that the mechanism governing backflow differs between the fuel and oxidizer states within each manifold, making the oxidizer manifold more susceptible to greater backflow of combustion gases.
- IV. Although the peak pressure cannot be fully captured owing to the 2 kHz sampling rate of the pressure sensor, a trend is observed where longer durations until re-ignition correspond to higher peak pressures. This correlation suggests that the peak pressure is sensitive to the volume of fuel accumulated in the combustion chamber prior to the oxidizer's transition back to liquid-phase injection.
- V. As the intensity of pressure increase resulting from the hard start decreases, the volume of combustion gas backflow into the MON-3 manifold also reduces. Eventually, when backflow was almost entirely suppressed, the system transitioned to stable combustion.

The critical factor to consider is that the presence or absence of backflow into the fuel manifold is influenced by the fluctuations in pressure within the supply system. These fluctuations, in turn, significantly impact the conditions conducive to multiple ignitions. Variations in pressure fluctuations of the supply system are caused by variations in the propagation speed of pressure waves within the liquid owing to the dissolution of the pressurizing gas into the propellant. In some spacecraft systems, it is unavoidable for pressurizing gas to dissolve into the propellant. Therefore, understanding its impact through ground testing is considered extremely important.

Furthermore, it is necessary to evaluate individually whether the situations depicted in Figure 5–6 could occur in flight conditions. First, the magnitude of the inlet pressure (PIF) drop associated with the opening of the propellant valve depends on the pressure propagation speed within the propellant. Additionally, the time history of PIF in Figure 5 captures vibrations near 10 Hz, which correspond to water hammer responses within the flow path piping. During the pressure measurement tests, vibrations of approximately 15 Hz were recorded, suggesting higher pressure propagation speeds compared to the visualization tests, where approximately 10 Hz vibrations were observed. Both the rate of pressure drop and water hammer responses appear to reflect variations in the pressure propagation speeds within the propellant, likely attributable to differences in the concentration of dissolved pressurizing gas. In cases where the PIF

time history suggests a higher amount of dissolved gas, the occurrence of multiple ignitions has been observed. In actual flight environments, from launch to orbital operations, the maximum amount of pressurizing gas can dissolve into the propellant. Therefore, ground firing tests must be designed considering this scenario. However, during ground tests, piping lines that were not present during the flight, such as the drain line shown in Figure 2, were installed. The water hammer responses observed in the PIF are influenced by these additional piping lines, which do not exist in flight conditions. Therefore, the pressure drop conditions at the time of ignition during ground tests cannot accurately replicate the dynamics of actual flight conditions. Addressing this discrepancy through ground testing exclusively presents significant challenges; thus, 1D-CFD simulations must be actively utilized to accurately estimate the water hammer responses in the supply system.

Table 1: Time required for a re-impinger	ement
--	-------

		Impinging element		Film Cooling	
	_	MON-3	Hydrazine	Hydrazine	
Flow velocity	m/s	13.08	12.63	12.63	
Orifice length	mm	1.16	0.92	0.98	
Time required to pass through	ms	0.09	0.07	0.08	
Distance to the impinging point	mm	1.62	2.23	2.64	
Time required to pass through	ms	0.12	0.18	0.21	
Total time	ms	0.21	0.25	0.29	

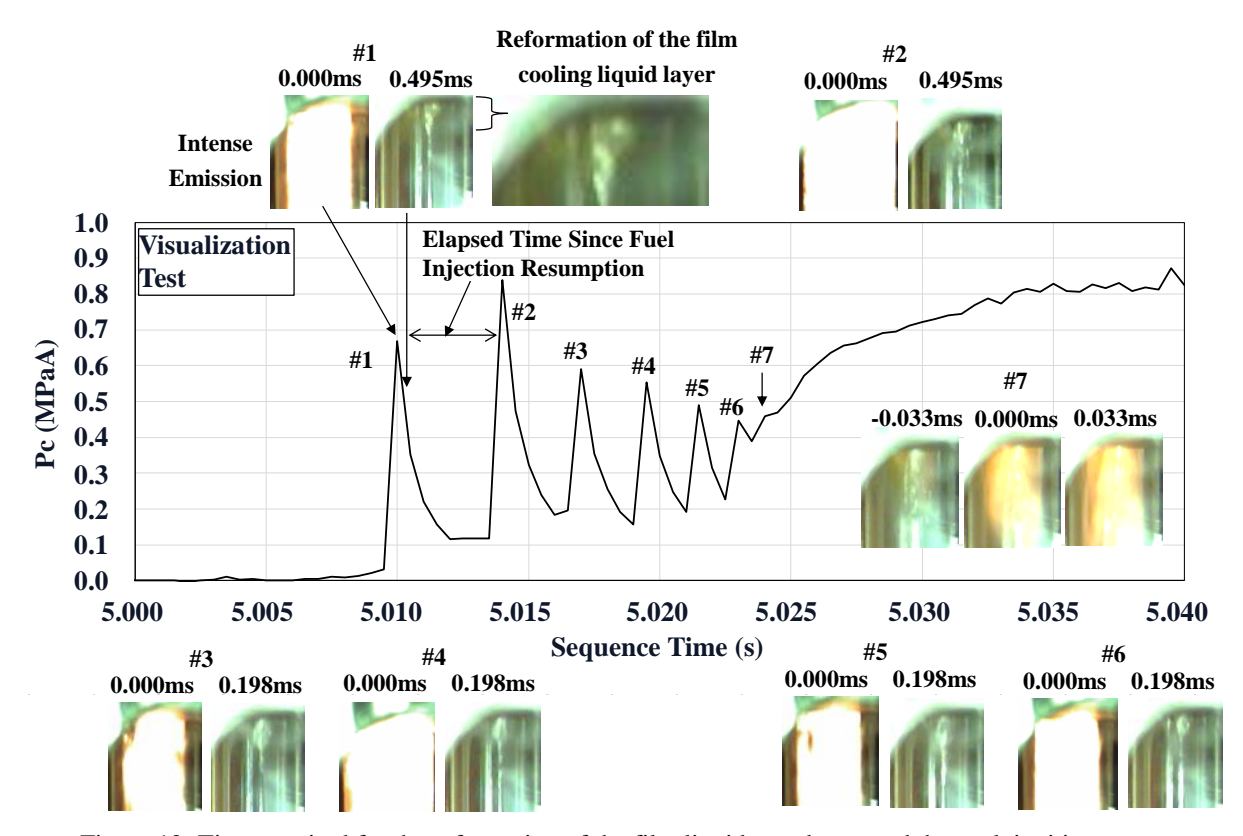


Figure 12: Time required for the reformation of the film liquid membrane and the peak ignition pressure.

5. Conclusion

In a bipropellant impinging combustion chamber operating in a vacuum, the flow path is initially in a vacuum state during the initial ignition timing. As a result, when MON-3, which possessed a high vapor pressure, entered the injector, vapor generated by flash boiling filled the manifold. This was followed by the onset of gas-phase-dominant injection, eventually increasing the liquid-phase component. This leads to the impingement of the liquid phase of the oxidizer with the liquid phase of the fuel, which had already initiated liquid-phase injection, culminating in ignition. Considering the dissolution of pressurizing gas into the propellant, the change in pressure propagation speed affects the supply pressure fluctuation caused by opening and closing of the propellant valve. If the engine initiates at a timing when the inlet pressure immediately upstream of the propellant valve drops significantly, there is a possibility of repeated abrupt ignitions and delayed transition to steady combustion. This scenario led to a prolonged delay in engine startup. The timing of the transition from a hard start to stable combustion is believed to be closely associated with the resolution of the gas-liquid two-phase state within the oxidizer manifold. From a design perspective, the minimization of the manifold volume to accelerate the transition to liquid-phase injection is important. Furthermore, the injection pressure differential should be sufficiently high to mitigate the risk of backflow associated with hard starts.

In spacecraft equipped with similar systems, changes in supply pressure responsiveness owing to the presence of dissolved pressurizing gas are anticipated. Notably, an increase in ignition delay time during pulsed operation could hinder the achievement of the required impulse, potentially compromising spacecraft attitude control or landing operations [3]. Therefore, combustion tests should be conducted under conditions that simulate the effects of dissolved gas anticipated in spacecraft during ground testing. Furthermore, a thorough evaluation of the differences in supply system design between ground tests and spacecraft should be performed through numerical analysis.

6. Future work

The variations in the behavior of the inlet pressure observed in Figure 5-7 are believed to be influenced by differences in the pressure propagation speed within the liquid which is attributed to the varying amounts of pressurizing gas dissolved in the propellant. As shown in Figure 2, the supply system utilized for firing test includes components such as flow meters, pressure conduits branching off from main pipelines, drain lines, GN2 purge lines, and orifices for flow adjustment. These structural elements, such as changes in flow paths and pipe branches, can create localized lowpressure regions. Such localized pressure drops may lead to the precipitation of the pressurizing gas, typically helium, dissolved in the propellant, resulting in the formation of microbubbles within the branch pipes. While the gas in these branch pipes remains in equilibrium with the supply pressure and generally does not significantly disrupt the stable propellant flow, the dynamics change when the propellant valve opens to initiate the combustion process. As the propellant flows from the valve into the downstream injectors, the upstream propellant begins to move downstream, causing a decrease in pressure within the pipes. If there are fewer bubbles within the branch pipes, the pressure in the pipes will quickly decrease as the propellant moves. Consequently, the differential pressure driving the propellant toward the injector decreased rapidly, leading to a decrease in the instantaneous flow rate. Conversely, if more bubbles are present within the branch pipes, their expansion in response to the surrounding pressure drop can mitigate the overall pressure decrease within the pipes. As a result, the differential pressure between the injector and the supply side remains relatively high, thereby mitigating the reduction in instantaneous flow rate.

Achieving this requires efforts to quantify the amount of pressurizing gas dissolved in the propellant, which will be a key focus of future research. Developing methodologies to measure and analyze dissolved gas levels will enable a deeper understanding of the impact of pressurizing gas on system performance and help refine testing protocols for more accurate simulation of space operation.

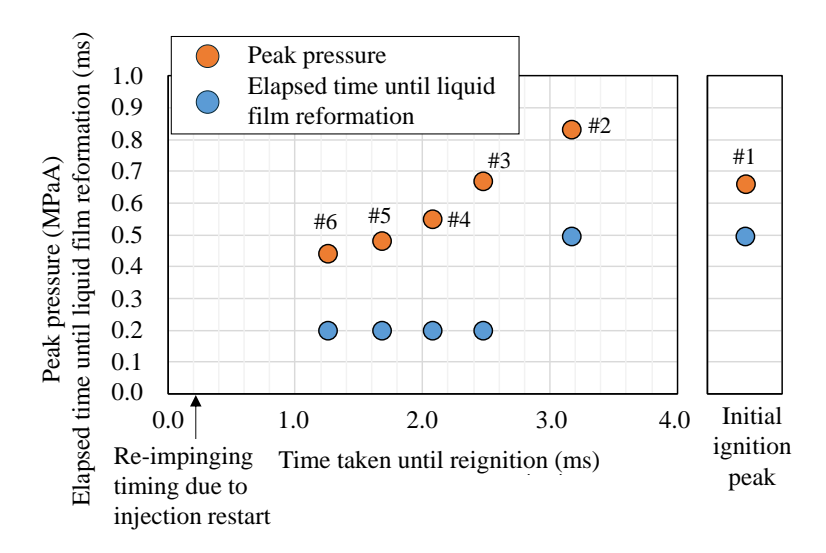


Figure 13: Elapsed time until re-ignition, elapsed time until the reformation of the film liquid membrane, and peak pressure.

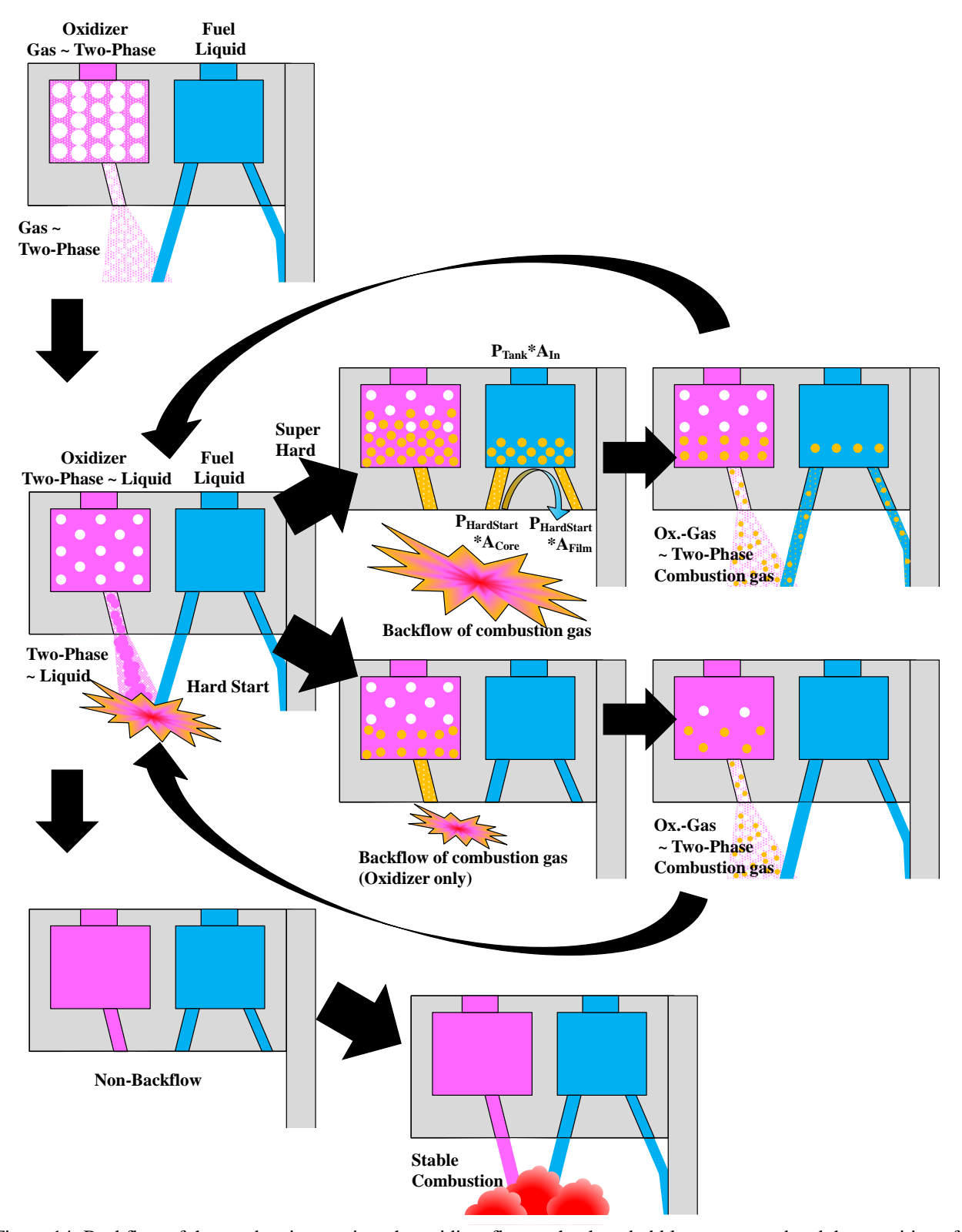


Figure 14: Backflow of the combustion gas into the oxidizer flow path where bubbles are trapped and the repetition of liquid-phase injection.

References

- [1] P.G. Sutton, History of liquid propellant rocket engines in the United States, *J. Propuls. Power* 19 (6) (2003) 978–1007.
- [2] S. Takata, H. Sasaki, T. Fukatsu, K. Sugimori, The compatibility evaluation method of the 500N & 120N Japanese Bi-propellant thrusters with the HTB system & operation design, In: *Trans. JSASS Aerospace Tech. Japan*, 12 (29) (204) 7–15.
- [3] T. Kato, et al., System firing test for the propulsion system for MMX program, In: 9th Space Propulsion Conference (2024) 099
- [4] M. Yoshiki, M. Naoki, T. Yousuke, N. Tomomi, Investigation on suppression of hard-start phenomena in hypergolic bipropellant engine, *J. Propuls. Power* 41 (1) (2025) 72–81. https://doi.org/10.2514/1.B39522.
- [5] B.V. Prashanth, O. Lars, F. Michael, M. Mesa, B. Daudi, Pulse performance analysis of a 45 Newton additively manufactured bipropellant thruster, *J. Propuls. Power* 37 (6) (2021) 832–841. https://doi.org/10.2514/1.B38326.
- [6] F. Go, D. Yu, I. Chihiro, S. Daijiro, T. Nobuhiko, F. Katsumi, Visualization of pulse firing mode in hypergolic bipropellant thruster, *J. Propuls. Power* 36 (5) (2020) 677–684. https://doi.org/10.2514/1.B37637.
- [7] M. Yoshiki, I. Shigeyasu, T. Yousuke, Hypergolic propellant ignition phenomenon associated with two-phase oxidizer flow injection, *J. Propuls. Power* 30 (5) (2014) 1399–1409. https://doi.org/10.2514/1.B35203.
- [8] Y. Daimon, K. Tominaga, G. Fujii, T. Nagata, Y. Matsuura, Y. Kano, E. Uchiyama, One-dimensional modeling of ignition timing for hypergolic bipropellant thrusters. In: *Aerospace Europe Conference*, 2023-10th EUCASS-9th CEAS, (2023).
- [9] K. Tominaga, Y. Daimon, G. Fujii, T. Nagata, Y. Matsuura, Y. Kano, E. Uchiyama, Estimation of hard start mechanism by visualization test of hypergolic bipropellant thruster. In: *Aerospace Europe Conference*, 2023-10th EUCASS-9th CEAS, (2023).
- [10] D.T. Campebell, et al., Reactive stream separation photography, AIAA J. 9 (9) (1971).